Mater. Res. Soc. Symp. Proc. Vol. 998 © 2007 Materials Research Society 0998-J05-06

Pulsed Laser Deposition of Chromium Oxides: Substrate Effects

Helia Jalili, Nina Heinig, and K. T. Leung
Departments of Physics and Chemistry, University of Waterloo, Waterloo, N2L 3G1, Canada

ABSTRACT

Pulsed Laser Deposition (PLD) was used to grow chromium oxides (CrO_x) on MgO(100), Al_2O_3(0001), $SrTiO_3$(100), $LaAlO_3$(100), and Si(100) under different growth conditions, including substrate temperature, O_2 pressure, and laser fluence. SEM, AFM and XRD measurements show that various phases of CrO_x films with different morphologies could be obtained on different substrates under the same growth conditions. Half-metallic CrO_2 needle-like nanostructured films were only observed on MgO(100) under a special set of conditions.

INTRODUCTION

Chromium oxides are interesting materials because of their technological applications as catalysts, gas sensors, dehydrogenation and protective layers for preventing oxidation [1,2,3,4]. In the case of CrO_2, its special magnetic and electrical properties have attracted a lot of recent attention. CrO_2 is ferromagnetic at room temperature, with a Curie temperature T_C=395 K. Band structure calculations indicate the half-metallic character of CrO_2 [5]. Spin- and energy-resolved photoemission data further show nearly 100% spin polarization for electrons with binding energies of 2 eV below the Fermi energy [6], suggesting CrO_2 as a promising candidate for spintronic applications [7,8,9]. Furthermore, in order to achieve the higher magnetic switching ratio by using the spin effects, it is crucial to prevent scattering during extraction of polarized spins. The development of preparation methods for defect-free multilayer films with high-quality interfaces is therefore of special importance to the fabrication of spintronic devices.

The metastable nature of CrO_2 at room temperature makes its synthesis difficult. Thermal decomposition of CrO_3 under a high oxygen pressure and chemical vapour deposition (CVD) methods are commonly used to grow CrO_2 films, with successful epitaxial growth demonstrated only on single-crystalline TiO_2 substrates [10,11,12,13,14]. PLD is a particularly powerful film growth technique because it enables the formation of metastable phases under non-equilibrium thermodynamic conditions. Furthermore, multilayer films and complex materials can also be obtained in situ by using different targets and feed gases, which is an important advantage in device fabrication. In the present work, we investigate the use of the PLD technique for the growth of a single-phase CrO_x film (particularly CrO_2), with focus on the nature of the resulting nanostructured films grown on different substrates, including MgO(100), Al_2O_3(0001), $SrTiO_3$ (100), $LaAlO_3$(100), and Si(100). Our goal is to develop a set of optimized growth conditions for producing a high-quality film by systematically varying the substrate temperature, the O_2 pressure, the laser fluence, and the target-to-substrate distance. Unlike the previous PLD studies that did not produce a single-phase CrO_x film [15,16], the present work shows that single-phase CrO_x films could be obtained for the first time on MgO(100) under a narrow set of conditions.

EXPERIMENTAL DETAILS

The PLD experiments were conducted in a turbomolecular-pumped NanoPLD system (manufactured by PVD Products) with a base pressure better than 5×10^{-7} torr. The system was equipped with multiple target holders and a substrate holder with a maximum growth temperature of 900°C. A 248-nm excimer laser with a laser fluence of 350-550 mJ/pulse was used to ablate the Cr metal target (99.95% purity, 1 inch diameter) at a repetition rate of 10 Hz. Oxygen was introduced into the chamber by a variable leak valve to a typical growth pressure of 10-400 mtorr. The use of higher substrate temperature, laser fluence and O_2 pressure is found to be important to achieving a single-phase film. The present system allows for film growth at higher temperatures and higher oxygen pressures than that have been previously attempted [15,16]. The substrates (5×10 mm^2, or 10×10 mm^2) used in the present work were cut from wafers of MgO(100), $SrTiO_3$(100), and $LaAlO_3$(100) substrates (MTI), and of Al_2O_3(0001) and Si(100) (University Wafers, all with 99.99% purity). The morphology and topography of the as-grown films were characterized by using scanning electron microscopy (SEM, LEO FESEM-1530) and atomic force microscopy (AFM, Digital Instruments Nanoscope IV), respectively, while the corresponding crystal structure was analyzed by high-resolution X-ray diffraction (XRD, PANAlytical X'Pert Pro MRD).

RESULTS AND DISCUSSION

Morphology

Various growth conditions have been attempted to develop a homogenous, single-phase CrO_x film. Of these experiments, we found that single-phase CrO_x films were more readily obtained at substrate temperature of 480°C, 400 mtorr O_2 pressure and laser fluence of 550 mJ/pulse. Except for the film grown on Si(100) that appears to be silvery black in colour similar to that of bare Si, the resulting films obtained on Al_2O_3(0001), $SrTiO_3$(100), and $LaAlO_3$(100)

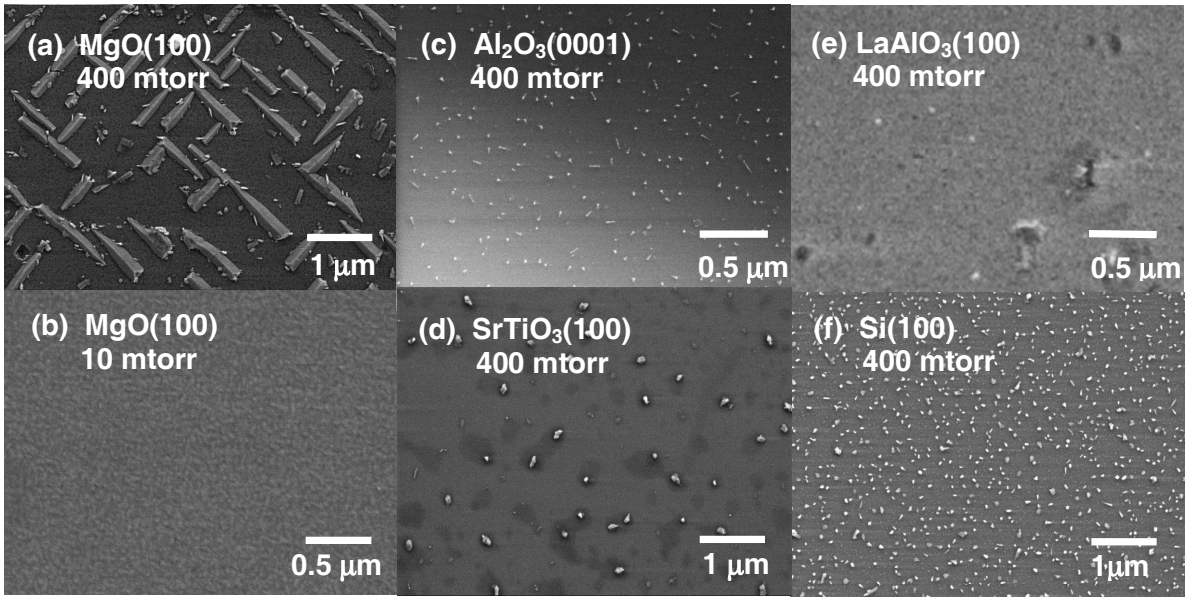

Figure 1: SEM images of CrO_x grown on MgO(100) with O_2 pressure of (a) 400 mtorr and (b) 10 mtorr, and on (c) Al_2O_3(0001), (d) $SrTiO_3$(100), (e) $LaAlO_3$(100) and (f) Si(100) with O_2 pressure of 400 mtorr, all at 480°C and with 550 mJ/pulse laser fluence.

are brownish in colour while that on MgO(100) appears grayish. Figure 1 shows the corresponding SEM images of the as-grown CrO_x films [17] on different substrates at the aforementioned conditions. Except for the Si(100) sample, silver paste was applied to the side of all of the other (insulating) samples to minimize the effect of charging. For the insulating samples, we show in Figure 2 their corresponding AFM images in order to better illustrate their morphologies. Evidently, needle-like nanostructures with an average size of 300 nm (wide) × 1-2 μm (long) and 30-40 nm in height (Figure 2a) are found. Furthermore, these needles are distributed in an orthogonal cross pattern (Figures 1a, 2a), suggesting that these nanostructures are epitaxially grown with respect to the surface registry of the MgO(100) substrate at 400 mtorr O_2 pressure. However, at a lower O_2 pressure of 10 mtorr (Figure 1b) and also at 100 mtorr (not shown), the as-grown film appears to be smooth and devoid of nanostructures. It should be noted that the films obtained at a lower O_2 pressure (10 mtorr, 100 mtorr) on MgO(100) are found to be yellow-green in colour. For all other substrates, smooth films decorated with nanoparticles of various sizes and shapes and number densities are observed. In particular, randomly oriented nanoparticles of 10-30 nm in size and nanorods with a typical length of 100 nm are found on Al_2O_3(0001) (Figures 1c, 2b) and Si(100) (Figure 1f). For $SrTiO_3$(100) (Figures 1d, 2c) and $LaAlO_3$(100) (Figures 1e, 2d), the nanoparticles are generally less dense, larger (100-300 nm) and irregular in shape.

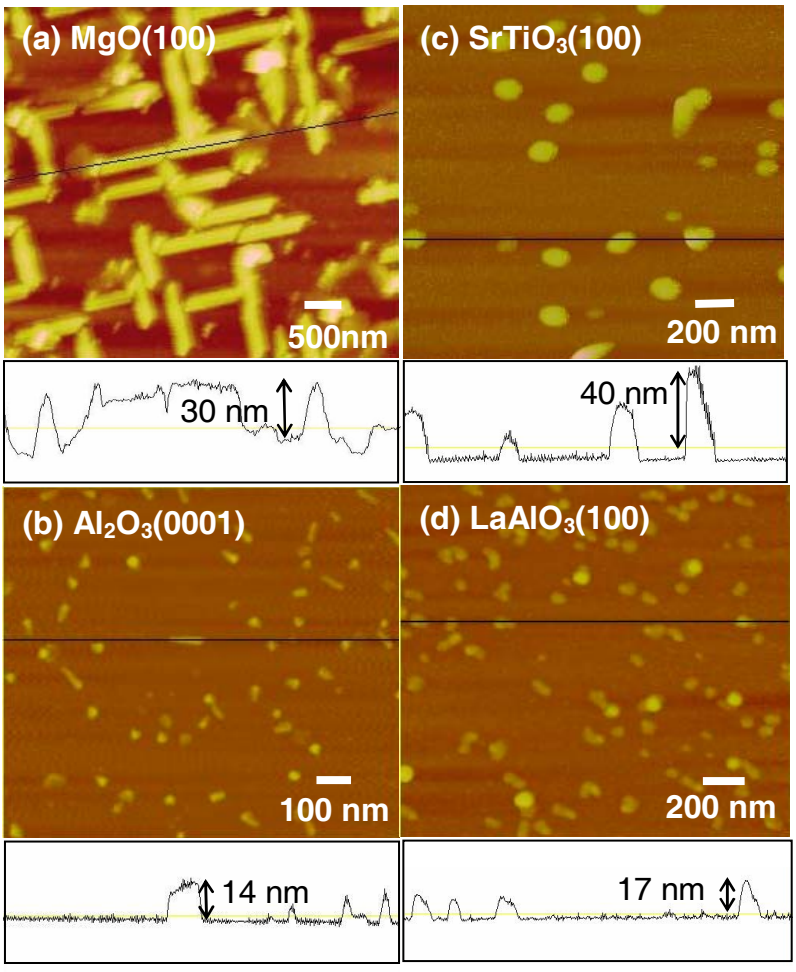

Figure 2. AFM images of CrO_x nanostructured films grown on (a) MgO(100), (b) Al_2O_3(0001), (c) $SrTiO_3$(100), and (d) $LaAlO_3$(100) at 480°C with O_2 pressure of 400 mtorr and 550 mJ/pulse laser fluence. The topography line scan of each image is also shown in the panel below the respective AFM image.

Crystal structure analysis

To further characterize the nature of CrO_x and their crystallinity, we collected high-resolution XRD data for all the samples shown in Figure 1. For the Al_2O_3(0001) (Figure 1c), $LaAlO_3$(100) (Figure 1e), and Si(100) samples (Figure 1f), no features other than the substrate peaks are observed, despite the presence of the discernibly visible films on the substrates. This suggests that the as-grown films are amorphous (or extremely thin). For the MgO(100) samples, the corresponding XRD patterns reveal additional features attributable to CrO_2 (Figure 3a) and Cr_2O_3 stressed films (Figure 3b) grown with O_2 pressures of 400 mtorr and 10 mtorr, respectively. For the sample grown on $SrTiO_3$(100) with 400 mtorr O_2 pressure, weak features attributable to CrO_3 and Cr_3O_4 (Figure 3c) are evident. At an O_2 pressure of 100 mtorr, no Cr related features are observed for the brownish film on the $SrTiO_3$(100) substrate.

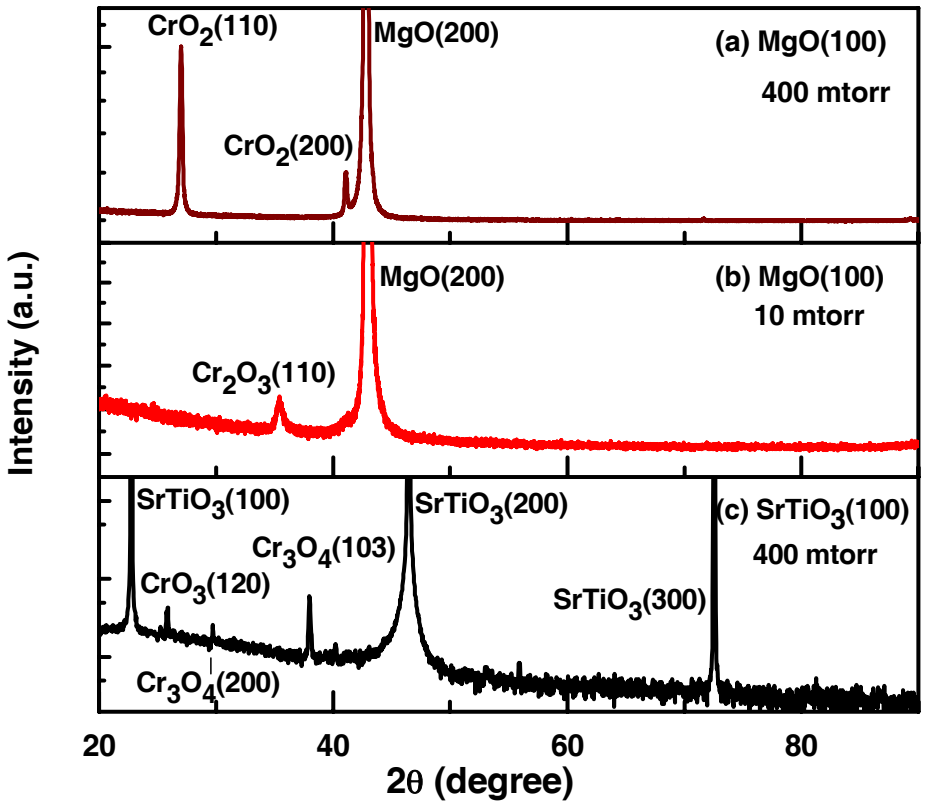

Figure 3: (θ–2θ) scan of CrO_x nanostructured films grown on MgO(100) with O_2 pressure of (a) 400 mtorr and (b) 10 mtorr, and on (c) $SrTiO_3$(100) with O_2 pressure of 400 mtorr, all at 480°C and 550 mJ/pulse laser fluence.

In Table 1, we show the space group and lattice parameters of the substrates and possible chromium oxide films [18]. Evidently, all three lattice parameters of CrO_2 closely match with those of TiO_2, while all but the c parameter match with those of MgO. The earlier CVD studies on CrO_2 epitaxially grown on TiO_2 [12,19,20] indicate that the as-grown CrO_2 film consists of well-defined needle structures, in close resemblance to the needle structures on MgO shown in Figure 1a. The presence of the observed needle structures on MgO in the present case is therefore in accord with the closely matched a and b lattice parameters between CrO_2 and MgO. At the lower O_2 pressure, the formation of Cr_2O_3 is not surprising due to the insufficient amount of oxygen present to allow the stoichiometric formation of CrO_2. The very weak intensity of the Cr_2O_3 feature observed in the XRD pattern (Figure 3b, note log scale) suggests that this may be due to randomly aligned crystalline precipitates, as suggested by the nanoparticles observed in the corresponding AFM image (not shown). In the case of $SrTiO_3$, we observe both Cr_3O_4 and CrO_3 peaks, also with very weak intensities.

Table 1. Lattice parameters of selected substrates and chromium oxides.

Material	**Space Group**	**Lattice Parameters**		
		a (Å)	**b (Å)**	**c (Å)**
Cr	Im-3m	2.9	2.9	2.9
Cr_3O_4	141/amd	6.1	6.1	7.5
Cr_2O_3	R-3c	4.9	4.9	13.6
CrO_2	**P42/mnm**	**4.41**	**4.41**	**2.91**
CrO_3	Ama2	5.7	8.5	4.8
TiO_2	**P42/mnm**	**4.59**	**4.59**	**2.95**
MgO	**Fm-3m**	**4.21**	**4.21**	**4.21**
Al_2O_3	R-3c	4.76	4.76	13
$SrTiO_3$	Pm-3m	3.90	3.90	3.90
$LaAlO_3$	R-3m	5.36	5.36	13.11
Si	Fd-3m	5.43	5.43	5.43

CONCLUSIONS

The pulsed laser deposition method was found to be a versatile technique to grow CrO_x nanostructured films using Cr metal as the target on several different substrates, including MgO(100), Al_2O_3(0001), $SrTiO_3$(100), $LaAlO_3$(100), and Si(100). The CrO_x films obtained on most of the substrates are found to be either amorphous [Al_2O_3(0001), $LaAlO_3$(100), and Si(100)] or consisting of more than a single phase [$SrTiO_3$(100)], or both. A single-phase nanostructured film of epitaxially grown CrO_2, decorated with the characteristic needle morphology, was found only on MgO(100). The present work also shows that the use of high O_2 pressure and high laser fluence is essential to the production of these novel needle nanostructures.

ACKNOWLEDGEMENTS

This work was supported by the Natural Sciences and Engineering Research Council of Canada. We thank Xiaojing Zhou, Liyan Zhao, Michel Thiam and Joel Pariag for their technical assistance and helpful discussions.

REFERENCES

1. M. P. McDaneil, *Catal*. 33, 47 (1985).
2. B. K. Miremadi, R. C. Singh, Z. Chen, S. Roy Morrison, K. Colbow, *Sensors Actuators* B 21, 1 (1994).
3. M. W. Mensch, C. M. Byrd, D. F. Cox, *Catal. Today* 85, 279 (2003).
4. R. O. Adamas, *J. vac. Sci. Technol. A* 1, 12 (1983).
5. K. Schwartz, *J. Phys. F: Met. Phys*. 16, L211 (1986)
6. K. T. Kamper, W. Schmitt, G. Gntherodt, R. J. Gambino, *Phys. Rev. Lett*. 59, 2788 (1987).
7 . A. Barry, J. M. Coey, M. Viret, *J. Phys.: Condens. Matter* 12, L173 (2000).
8. X. W. Li, A Gupta, G. Xiao, *Appl. Phys. Lett.* 75, 713 (1999).
9 . J. M. Coey, M. Venkatesan, *J. Appl. Phys.* 91, 10 (2002).
10. B. Kubota, E. Hirota, *J. Phys. Soc. Jpn.* 16, 345 (1960).
11. S. Ishibashi, T. Namikawa, M. Satou, *Mat. Res. Bull*. 14, 51 (1979).
12. A. Gupta, J. Z. Sun, *J. Magn. Magn. Mater.* 200, 24 (1999).
13. W. J. DeSisto, P. R. Broussard, T. F. Ambrose, B. E. Nadgorny, M. S. Osofsky, *Appl. Phys. Lett.* 76, 25 (2000).
14. H. A. Bullen, S. J. Garrett, *Chem. Mater*. 14, 243 (2002).
15. M. Shima, T. Tepper, C. A. Ross, *J. Appl. Phys.* 91, 7920 (2002).
16. D. Stanoi, G. Socol, C. Grigorescu, F. Guinneton, O. Monnereau, L. Tortet, T. Zhang, I. N. Milailescu, *Mater. Sci. Eng. B* 118, 74 (2005).
17. It should be noted that while the SEM (or AFM) images appear to show that the deposited films to be not continuous, it is not possible to determine whether their respective nanostructures are not on top of a "wetting" layer of a few atoms thick (especially given their colours over the substrates). As such, the word "film" is used somewhat ambiguously here, and it refers to the nanostructured overlayer that may or may not be continuous.
18. PDF22004 (Highscore).
19. N. Umada, H. Yanagihara, A. Hatanaka, E. Kita, *Jap. Soc. Appl. Phys.* 44, 6538 (2005).
20. T. Yu, Z. X. Shen, J. He, W. X. Sun, S. H. Tang, J. Y. Lin, *J. Appl. Phys*. 93, 7 (2003).